

ORIGINAL INNOVATION

Open Access



Damage characterization and resilience optimization of reinforced concrete bridge piers under vehicle impact

Suman Roy^{*} , Ikwulono D. Unobe and Andrew Sorensen

^{*}Correspondence:
sumanroy74@gmail.com

Department of Civil
and Environmental Engineering,
Utah State University, Logan, UT
84322, USA

Abstract

Vehicle impact creates a dynamic loading condition at high strain rate exhibiting a unique interaction with the resisting structural members' material properties. This interaction results in an increase in the material's strength properties, a behavior captured in analysis via the computation of a strength factor known as the dynamic increase factor (DIF). In reinforced concrete (RC) bridge piers, the concrete cover receives the initial impact from the vehicle, causing damage to this exterior surface. This makes the DIF related to the concrete material (i.e., the compressive DIF) particularly important in this initial phase of the crash scenario; thus, requiring an in-depth analysis into its effect on the performance of the pier during and after the impact event. This study initiates an investigation into the influence of the compressive DIF on the performance of RC piers under impact from vehicles classes. Of particular interest is estimating a post impact residual capacity for the pier, while also determining concrete strength parameters (compressive strength) that offers a good tradeoff between the shear capacity which primarily resists the impact loads, and the axial capacity which controls the principal serviceability of the pier. The resulting analyses, using a representative test pier, show that an optimal compressive strength of concrete will minimize loss in the residual capacity of the pier. The effect of the compressive DIF on other important design parameters, i.e., bond strength and development length is also scrutinized. This study will aid forensic structural engineers in scrutinizing the post impact concrete behavior and serviceability.

Keywords: Vehicle impact, Damage index, Deterministic and resistance reduction method in determining shear and axial residual capacities, Bond strength, Development length

1 Introduction

Collisions between vehicles and traditional reinforced concrete (RC) bridge piers have a significant influence on the safety and continued serviceability of the bridge structures, with research indicating collisions between vehicles and bridge piers are the second leading cause of bridge failures in the United States (Cook 2014; Wardhana and Hadipriono 2003). Impact to bridge piers from high-speed vehicle causes damage to the supporting structure, ranging from minimal damage such as localized cracking of the concrete at

the impact location to severe damage, such as pier fracture, support failure and bridge collapse. With such wide variations in the possible extent of damage, in-depth analyses of the pier after impact to certify it for continued service is necessary. Scrutiny of the severity of damage to decide on whether to keep the bridge piers in service has long been mandatory, with collision analyses in practice normally employing static analysis (Joshi and Gupta 2012). Investigations into characterizing the damage to bridge piers has been the focus of several studies. These studies have shed a light on the behavior of RC bridge pier under impact including increases in the material properties under high strain rate loading (Malvar and Crawford 1998), estimation of the dynamic shear capacity of an RC pier and the demand from colliding vehicles (Sharma et al. 2012) and characterization of the damage suffered during impact via a damage index (Auyeung et al. 2019; Zhou and Li 2018a). Unfortunately, little attention has been given to the role of concrete in this loading scenario especially in post impact transfer of load, estimating the damage level, probability of failure, and identifying an optimized combination of concrete and steel to enhance the performance of the piers under horizontal impact load.

At high strain rates of loading, the apparent strength of concrete increases significantly. This apparent increase in concrete strength is evaluated by computing a dynamic increase factor (DIF) and scaling the compressive strength of the concrete by this factor. The dynamic increase factor (DIF) which is basically a ratio of the dynamic to static compressive strength has been considered in this study to investigate the optimized concrete strength that is suitable in withstanding the specific impact scenarios, can be expressed as a function of strain rate and collision parameters leading to the deformation of the pier (Malvar and Crawford 1998). Concrete DIF has been utilized to investigate conservatively for different vehicle impact scenarios to evaluate post impact residual capacities in terms of concrete resilience. Deformation of a reinforced concrete (RC) pier during and post impact is a complex phenomenon. During a collision event, the RC pier experiences a high strain rate of loading, primarily in the transfer of energy (Roy and Sorensen 2021a) from the vehicle into the concrete surface of the pier. This could lead to crack propagation (Roy and Sorensen 2021b) followed by significant bond failure in the bond between the concrete and reinforcing steel, and eventually plastic deformation after forming plastic hinge near the impact location (Kowalsky 2000). The bond strength (u) is a useful property of the reinforced concrete (RC) as it defines the quality of bond between the disparate materials (concrete and steel), and by extension their ability to act as a cohesive unit. Equally important is the necessary development length (l_d) of the reinforcing steel, which is required to prevent pullout. The apparent increase in the compressive strength of the concrete at high strain rates leads to increases in the bond strength and a concurrent decrease in the required development length. This phenomenon seemingly enhances the resistance of RC piers to vehicular collisions and should be accounted for when estimating the post impact residual capacity of the traditional RC pier.

Quantification of damage to the pier is essential before retrofitting and rehabilitation to return it to service are carried out. The damage under impact load is identified using some parameters from the impact scenario, coalesced into a single parameter known as the damage index (λ). Characterizing the severity of damage to the structural member, the damage index (λ), is expressed as a ratio of the impact force and the dynamic shear

capacity of the pier which are in turn contingent upon the vehicle characteristics and subsequent pier behavior respectively (Zhou and Li 2018a). To quantify the damage (Shi et al. 2008) proposed, a relationship between the damage index and the residual capacity seem crucial with the initial design strength of the RC pier. Rearrangement of this relationship allows for the computation of a residual capacity for the pier using knowledge of the design parameters as well as the impact conditions. An important parameter for computing the damage index is the impact force. Deterministic analyses barely captures the risk and uncertainties involved in assessing the post impact non-linear dynamic behavior of RC piers (Roy et al. 2022). Difficulties in computing an exact impacting force due to its variation over the duration of impact, has led to the development of several models for estimating the impacting force as an equivalent static force. These models generally involve integrating the instantaneous impact force and normalizing this integrated force using different variables compared the different models and have determined that the local equivalent static force (LESF) model best captured the pattern of the impact force on the pier (Zhou and Li 2018a). However, in using this model to estimate the residual capacity, the variability of the design parameters as well as the parameters specifically administering the impact scenario are not considered.

To capture the variability of these parameters, a new factor for estimating the residual capacity is proposed. This factor, derived using the resistance reduction method (Thomas et al. 2018), is based on utilizing a reliability analysis to determine the effect of a loading scenario on a structural member. The reliability analysis results aid scrutinizing the function of parameters affecting the particular loading scenario exerted by a specific speed and weight of vehicle (Vehicle Class), all defined as random variables (Nowak and Collins 2012).

The objective of this study is to examine the contribution of concrete in resisting vehicular impact, particularly the effect of the high strain rate loading expected in the vehicle impact scenarios on the flexural and shear capacities of the representative circular RC bridge pier. As high strength concrete is brittle in nature and vulnerable to shear forces, and low strength concrete is vulnerable under flexure and axial compression, there is a need to determine an optimal concrete compressive strength to be used in bridge piers to minimize impact failure. The post impact performance of different concrete compressive strength is investigated to determine an optimal strength of concrete for resisting and withstanding the vehicle impact load. To understand the contribution of concrete in resisting impact load, bond strength and corresponding development length conforming bond characteristics are also studied. This study is carried out using different vehicle weights and travel speeds to produce various impact forces in order to come up with optimal and reliable concrete grade to be used safely and resiliently (Cao et al. 2019).

2 Deformation of concrete due to impact

Among reinforced concrete (RC) structural elements, columns are particularly susceptible to high strain rate impact from vehicle collisions. Impact as a result of collision, produces high peak resulting high strain rate (change in strain over change in time) of approximately 1000 s^{-1} leading to significant increase in concrete strength (Malvar and Crawford 1998; Shi et al. 2008). This increase in the strength of concrete due to dynamic impact is predicted using a dynamic increase factor (DIF) (Malvar and Crawford 1998).

Defined as the ratio between dynamic and static strength of concrete, the DIF is computed using the dynamic strength of concrete at a specific strain rate and is in turn used to determine the dynamic compressive strength of the concrete.

2.1 Dynamic increase factor in compression (CDIF)

Dynamic Increase Factor in compression (CDIF), is the ratio between the dynamic compressive strength at dynamic strain rate to static compressive strain rate at quasi-static strain rate, and is defined using the relationship as shown in Eq. 1 (Malvar and Crawford 1998).

$$CDIF = \frac{f_{cd}}{f_{cs}} = \left(\frac{\dot{\epsilon}_d}{\dot{\epsilon}_{cs}} \right)^{1.026\alpha} \text{ for } \dot{\epsilon}_d \leq 30s^{-1} \quad (1)$$

where: f_{cd} is the dynamic compressive strength at the dynamic strain rate $\dot{\epsilon}_d$, f_{cs} comprising static compressive strength as quasi-static strain rate $\dot{\epsilon}$ ($\dot{\epsilon} = f_{cd} / f_{cs}$) to compute dynamic increase factor (DIF) for concrete in a compression. The factor, α , is expressed in Eq. 2 (Malvar and Crawford 1998).

$$\alpha = \left[\frac{1}{5 + 9 * \left(\frac{f_{cs}}{f_{cu}} \right)} \right] \quad (2)$$

where: f_{cu} is the cube compressive strength of concrete and f_{cs} comprises the static compressive strength as already stated.

3 Determination of vehicular impact

Bridge piers are designed considering static load conditions for axial, shear, bond, and development length, with dynamic loads given little consideration. However, dynamic effects play a major role in some loading scenarios such as impact, blast, and seismic events. To evaluate the effects of impact loads on RC piers, the dynamic impact force is estimated as an equivalent static force as described in this section.

3.1 Dynamic force due to vehicular impact





Assuming the vehicle comes to rest without rebounding from the pier, the kinetic energy (E) equations is determined as the kinetic energy of the vehicle using Eq. 3 (Bathurst et al. 2008).

$$E = 0.5M_{veh}V^2 \quad (3)$$

where: M_{veh} represents the classification of weight of the impacting vehicle (AFDC 2018) as shown in Table 1, E is the impact energy of the vehicle, and V is the frontal impact velocity of the vehicle at impact.

The dynamic impact force (I_{dyn}) exerted by the vehicle on the pier is represented using the pressure from the impacting vehicle, the pier geometric dimensions and the duration of impact as shown in Eqs. 4, 5 and 6 (Vrouwenvelder 2000; Zhou and Li 2018a). An impact pulse representing the impact duration over the duration of impact is characterized using as half sine function with amplitude as the peak impact force. The half sine function is chosen to represent the impact pulse as it is characteristic of the behavior

Table 1 Classification of vehicle categories (AFDC 2018)

Vehicle Class	Picture	Description	Weight (lbs.) (kN)	Weight Used in Analysis (lbs.) (kN)
5		Medium Delivery Truck	26,000 (115.65)	26,000 (115.65)
6		Medium Duty Truck	34,000 (151.24)	34,000 (151.24)
7		Heavy Duty Truck	74,000 (329.16)	74,000 (329.16)
8		Semi-trailer Truck	80,000 (355.86)	80,000 (355.86)

of the impact over its duration. An averaged integration is then used to determine the equivalent static force occurring from the impact pulse. The averaged integration is done over a small window around the peak impact force to obtain a conservative estimate that accurately reflects the load transferred to the pier from the vehicle at the peak of the impact. The peak impact force is determined as a function of the kinetic energy (E) from the colliding vehicle, the geometric dimensions of the pier and the duration of impact (t) are as shown respectively in the Eqs. 4, 5 and 6 (Roy, S., Unobe, I., and Sorensen 2021; Zhou and Li 2018b).

$$I_{dyn} = \frac{\int_{t_d-0.025}^{t_d+0.025} I_r \sin\left(\frac{\pi t_d}{t}\right) dt}{0.05} \quad (4)$$

$$I_r = ((2 * 10^{-5} E) + 386.48) \left[\frac{I * L}{(a * b * c)} \right] \quad (5)$$

$$t = \sqrt{\frac{m}{k}} \quad (6)$$

where: I_{dyn} represents the frontal shock (force) due to impact, I_r is the peak reflected pressure (overpressure), t represents the impact duration, E is the kinetic energy absorbed by the impacted bridge pier, L is the unsupported length of the pier, a is the distance from the bottom of the pier to the point of impact, b is the distance from the top of the pier to the point of impact, and c is the perpendicular distance from the neutral axis (NA) of the cross section to the farthest point (extreme fiber) on the cross section of the pier, m is the weight of the impacting vehicle, and k is the vehicle frontal stiffness as shown in Fig. 1 (Mander et al. 1988; Roy, S., Unobe, I., and Sorensen 2021).

To quantify the damage resulting from impact to the RC pier, the residual capacity of the pier post impact can be determined. This residual capacity offers an insight into further serviceability of the pier, allowing decisions to be made on retrofitting/rehabilitation or possible replacement. The residual capacity is computed as a function of the design capacity and the damage occurring from the impact (Shi et al. 2008). Two methods are studied for use in quantifying the damage from impact; computing a damage

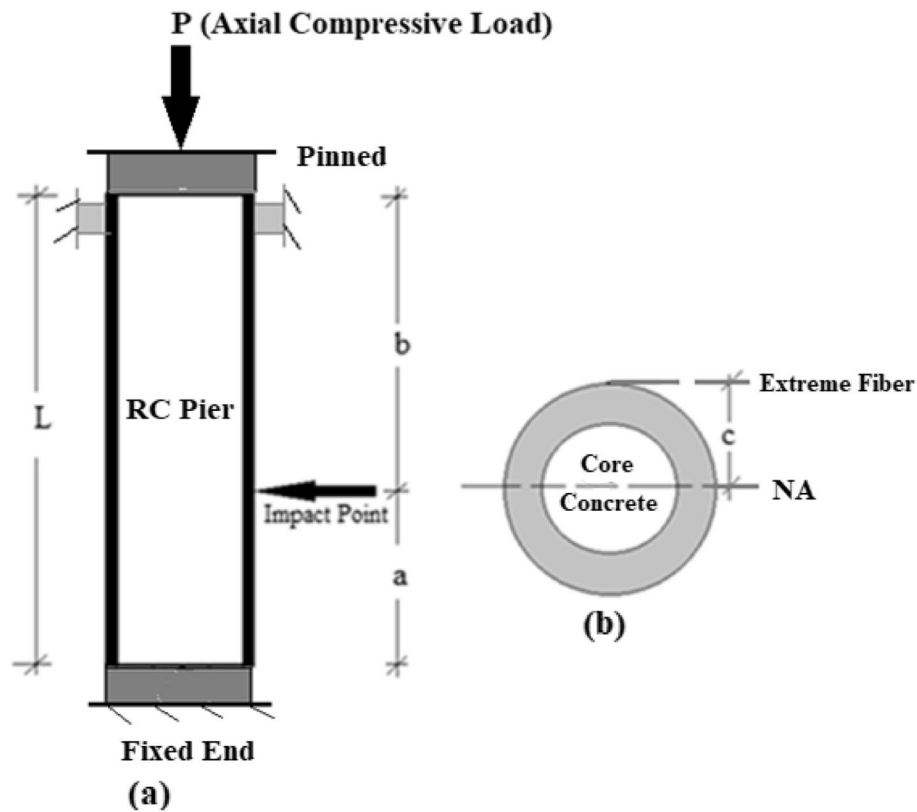


Fig. 1 Impact Location and Geometry of RC Bridge Pier (Roy et al. 2022)

index (Zhou and Li 2018a) and computing a resistance reduction factor (Thomas et al. 2018). End connections of the impacted pier are considered to be bottom end restrained from rotation, translation and deflection whereas the upper end is pinned. This is further shown precisely in the Fig. 1 (a) as well.

3.2 Damage indices

The damage of reinforced concrete material under impact load can be appraised using a damage index. Computed as a ratio of the equivalent static force from the impact to the shear capacity of the pier, the damage index (λ) is assessed as shown in Eq. 7 (Roy, S., Unobe, I., and Sorensen 2021; Zhou and Li 2018b).

$$\lambda = I_{dyn} / V_{dyn} \quad (7)$$

where: I_{dyn} is the peak vehicle dynamic impacted force, and V_{dyn} indicates the dynamic shear effect on concrete.

The dynamic shear (V_{dyn}) of the pier is a function of the strain rate behavior of the concrete material as encapsulated in the dynamic increase factor (CDIF) considering resiliency factor. Computed as shown in Eq. 8 (Feyerabend 1988; Malvar and Crawford 1998), the dynamic shear capacity offers an insight into the expected behavior of concrete under dynamic loading events.

$$V_{dyn} = CDIF * V_n \quad (8)$$

The relationship between the damage index and residual strength of the damaged column is shown in Eq. 9 (Shi et al. 2008).

$$\lambda = 1 - (L_{Residual}/L_{Design}) \quad (9)$$

where: $L_{Residual}$ is the residual strength for axial or shear of the damaged column after experiencing vehicular impact, and L_{Design} is the design axial or shear load carrying capacity of the undamaged reinforced concrete bridge pier as stated in ACI (ACI 2011).

Rearranging Eq. 9 allows for the determination of the residual strength of the damaged RC pier as shown in Eq. 10 (ACI committee 318 1985; Roy, S., Unobe, I., and Sorensen 2021).

$$L_{Residual} = (1 - \lambda) \cdot L_{Design} \quad (10)$$

3.3 Resistance reduction method

Any failure takes place when demand exceeds the capacity. Exceedance of the capacity or resistance in the function by the load or demand component results in a failure and vice versa (Nowak and Collins 2012). Mathematically modeled as shown in Eq. 11 (Spyrakos and Vlassis 2003), the probability of failure is a measure of the safety or otherwise of a structural member including the uncertainties in the load and resistance parameters that define its performance.

$$P_f = Pr[g(x) < 0] \quad (11)$$

where: P_f is the probability of failure, $g(x)$ is a performance or limit state function and x is a vector of all the random variables included in the limit state function.

Determined by integrating the limit state function over the region where the function is negative, the probability of failure is quite difficult to compute directly. As such, several methods have been developed to compute a reliability index for a structure or structural member which is then used to estimate the probability of failure. Converse to the probability of failure, the reliability index (β) is a measure of structural reliability which captures the inherent influence of parameter uncertainties (Der Kiureghian 2008). The reliability index (β) is modeled as the inverse of the tail probability function as shown in Eq. 12 (Ayyub and McCuen 2016; Nowak and Collins 2012).

$$P_f = \Phi(-\beta) \quad (12)$$

where: Φ is the standard normal cumulative function, β is the reliability index, and P_f represents the probability of failure.

The reliability index (β) is computed utilizing the Hasofer-Lind reliability method and using the procedure itemized below (Nowak and Collins 2012):

An appropriate limit state function is identified for the specific scenario. In this study, the limit state ratio is defined as the exceedance of the shear capacity by the dynamic impact force exerted by the impacting vehicle as shown in Eq. 13 (Roy et al. 2022).

$$g(x) = 1 - \lambda = 1 - \frac{I_{dyn}}{V_{dyn}} \quad (13)$$

Initial design points are assumed for all but one of the random variables and the limit state is solved at $g=0$ for the remaining random variable. The mean value of each random variable is a good initial assumption for the design point.

Reduced variates for each random variable are determined as shown in Eq. 14.

$$z_i^* = \frac{x_i^* - \mu_{x_i}}{\sigma_{x_i}} \quad (14)$$

where: z_i^* is the reduced variate of the i th variable, x_i^* is the design point, μ_{x_i} is the mean of the i^{th} random variable and σ_{x_i} is the standard deviation of the i^{th} random variable.

Partial derivatives of the limit state function with respect to each random variable are determined and multiplied by the standard deviation of each random variable and collected into a column vector G which is multiplied by (-1) .

An estimate of the reliability index (β) is then computed as shown in Eq. 15 and a column vector of sensitivity factors computed as shown in Eq. 16.

$$\beta = \frac{\{G\}^T \{z^*\}}{\sqrt{\{G\}^T \{G\}}} \quad (15)$$

$$\{\alpha\} = \frac{\{G\}}{\sqrt{\{G\}^T \{G\}}} \quad (16)$$

Reduced variates for new design points are then computed as shown in Eq. 17, followed by the computation of the corresponding design points as shown in Eq. 18.

$$z_i^* = \alpha_i \beta \quad (17)$$

$$x_i^* = \mu_{x_i} + z_i^* \sigma_{x_i} \quad (18)$$

The limit state function is then set to zero and solved for the remaining variable as done previously and the steps are repeated until convergence of the reliability index β and the design point x_i^* .

Notionally, the structural reliability of a system under sequential loading is defined by a fault tree analysis (Ayyub and McCuen 2016). This approach defines the probability of failure using the Bayesian framework for combining probabilities into a single defining probability, capturing the expected reduction in resistance to loading after a particular loading event and prior to the next. This has formed the basis of multi-hazard analysis allowing for a computation of the reliability indices and probabilities of failure of structures undergoing several independent loading scenarios.

A recently developed method to resolve some of the challenges with using the fault tree analysis is the resistance reduction method (Thomas et al. 2018). This method works to capture the reduction in capacity of a structure due to a loading event by utilizing the probability of failure of the structural member. A resistance reduction factor is computed and then used as a multiplication factor to adjust the structural capacity of a member after the loading event. This resistance reduction factor (ζ) is computed as the complement of the probability of failure (P_f) as shown in Eq. 19 (Thomas et al. 2018).

$$\zeta = 1 - P_f \quad (19)$$

where: ζ is the resistance reduction factor and P_f is the probability of failure of the structural member due to a specific loading event.

Alike the damage index, the resistance reduction factor can be used to effectively reduce the design capacity to a residual capacity by multiplying the factor by the design capacity, thus accounting for the damage incurred by the pier during the impact event.

3.4 Pier capacities in static load condition

Prior to computing the residual capacities, the design capacities in axial and shear for the representative RC pier are computed as specified in ACI (ACI 2011).

The design axial capacity (P_n) is computed as shown in Eq. 20 (Engineers 2013).

$$P_n = 0.85 * f'_c * (A_g - A_s) + \sigma_y * A_s \quad (20)$$

where: f'_c is the 28 days' compressive strength of the concrete in representative pier, σ_y is the yield strength of steel (60 ksi or 413.68 MPa), and A_g and A_s are the gross area of pier cross-section and total cross-sectional area of longitudinal (main) steel rebar, respectively.

The design shear capacity of the RC bridge pier is determined using Eq. 21 (AASHTO 2011).

$$V_{N,design} = V_c + V_s \quad (21)$$

where: V_c is the shear strength carried by the concrete and V_s is the transverse shear capacity.

The shear strength, V_c , is computed as shown in Eq. 22 (AASHTO M145-91 2008).

$$V_c = v_b [1 + 3P_{N,design}/f'_c] \bullet A_g \bullet A_e \quad (22)$$

where: A_g represents the gross cross-sectional area of the concrete in the pier and A_e is 80% of A_g , i.e., $A_e = 0.8 * A_g$, and v_b is the shear constant.

The shear constant (v_b) is determined using Eq. 23 (AASHTO M145-91 2008).

$$v_b = [0.0096 + 1.45\rho_t] \bullet (f'_c)^{1/2} \leq 0.03(f'_c)^{1/2} \text{ ksi} \quad (23)$$

where: ρ_t is the longitudinal steel ratio and $P_{n,design}$ represents the axial load capacity of the reinforced concrete pier.

The transversal shear capacity, V_s is computed using Eq. 24 (AASHTO M145-91 2008).

$$V_s = \pi/2 A_h \sigma_{yh} D' / s \quad (24)$$

where: A_h is the area of a single hoop or spiral, D' is the spiral or hoop diameter, s denotes the pitch of the helix, and σ_{yh} represents the yield stress of transverse reinforcing steel.

4 Results

In order to analyze the axial and shear strengths, bond capacities, and development length of the circular reinforced concrete bridge-pier, and its behavior during vehicular impact, a test column is analyzed (Ameli and Pantelides 2017). Several vehicle weights (Vehicle Classes 5 to 8) as shown in Table 1, as well as several impact velocities between 25 and 80 mph (15.53 km/hr and 49.71 km/hr) are considered for the impact scenarios.

The representative RC pier of 21 inches (0.53 m) diameter pier is examined for different vehicle impact scenarios using several concrete grades between 3 ksi, (20.68 MPa) to 10 ksi to (68.95 MPa) in this study. The height (unsupported length) of the pier is considered as 8.5 feet (2.6 m) with a uniform circular cross-section. Longitudinal (primary) reinforcement is provided by using steel re-bars with the specification of ASTM A706 having grade of 60 ksi (413.68 MPa). The pier has longitudinal reinforcement of (6) # 8 steel re-bars through its length, with a spiral (helical) shear reinforcement using # 4 steel (grade of 36 ksi or 248.21 MPa) re-bar @ 2–1/2 inches' (63.5 mm) vertical pitch. Bottom end of pier is fixed and the free end is restrained against deflection and rotation in all directions as shown in Fig. 1 (a) (Zhou and Li 2018a). The cross-section and reinforcement details of the representative pier are shown in Fig. 2 (a and b) (AASHTO 2011).

The reliability analysis requires design parameters to be treated as random variables and their statistical parameters (mean and standard deviations) as well as their distributions are used in determining the reliability index. Table 2 outlines the random variables and their distributions. The parameters for the geometric dimensions as well as the material properties are obtained from past studies as published in (Nowak and Collins 2012). The vehicle mass parameters are obtained from weigh in motion data for the state of Utah (Schultz and Seegmiller 2006) and the vehicle speed parameters from (Hwang and Nowak 1991). The pitch of the transverse reinforcement is assumed to remain constant and is not a random variable. Design variables comprising individual uncertainty parameters are given in Table 2.

A quasi-static strain rate of 30 s^{-1} is considered for the impact scenario (Malvar and Crawford 1998). Computations of the design axial and shear capacities at increasing concrete compressive strengths are carried out and the results plotted as shown in Fig. 3.

From Fig. 3, it can be observed that the design capacities in axial and shear relate with the concrete compressive strength in diametrically opposing ways. Higher

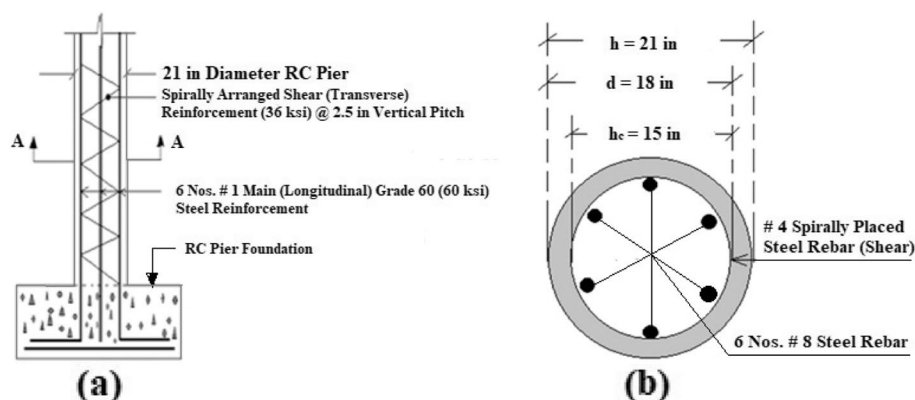
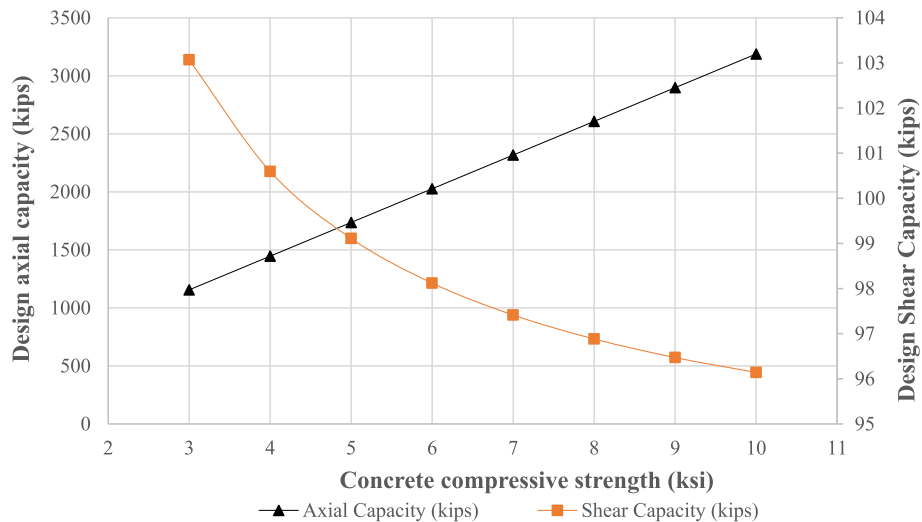


Fig. 2 a Representative RC bridge pier longitudinal section, and (b) Section A-A

Table 2 Design variables and their uncertainty parameters

No	Variables	Distribution	Mean	CoV	St. Dev	Units
1	Diameter of pier (d)	Normal	21.06 (0.53)	-	0.25 (0.006)	inches (m)
2	Height of pier (h)	Normal	102.06 (2.60)	-	0.25 (0.006)	inches (m)
3	Vehicle weight (m)	Normal	Varying	0.235	-	lbs (kN)
4	Vehicle velocity (v)	Lognormal	Varying	0.165	-	ft/s (m/s)
5	Core diameter (d_c)	Normal	18.06 (0.46)		0.25 (0.006)	inches (m)
6	Yield strength of transverse Reinforcement (σ_{yt})	Lognormal	45,300 (312.33)	0.116	5254.8 (36.23)	psi (MPa)
7	Compressive strength of concrete (f'_c)	Normal	Varying	0.18	-	psi (MPa)
8	Diameter of longitudinal reinforcement (d_l)	Normal	0.855 (0.021)	-	0.365 (0.009)	inches (m)
9	Yield strength of longitudinal reinforcement (σ_{yl})	Lognormal	67,500 (465.40)	0.098	6615 (45.61)	psi (MPa)
10	Diameter of transverse reinforcement (d_t)	Normal	0.48 (0.01)	-	0.365 (0.009)	inches (m)
11	Stiffness (k)	Normal	1,713,045 (300.00)	0.2	342,609 (60.00)	lb/in (kN/m)
12	Pitch (s)	Deterministic	2.5 (0.06)	-	-	inches (m)

**Fig. 3** Concrete compressive strength with design axial and shear capacities of RC pier

grades of concrete are more brittle, and hence more vulnerable to shear failure as a result of impact (Gomez and Alipour 2014). Increasing the compressive strength will result in increasing the axial capacity but reduces the shear capacity. An optimal compressive strength to balance both these design capacities can be selected as the intersection point on the graph in this case about 4.75 ksi (32.75 MPa). However, some insights are needed to scrutinize the concrete performance of the pier encountering the dynamic load incurred from vehicle impact.

4.1 Residual capacities using damage index method

Post impact residual capacities of RC bridge pier because of different vehicle weights and permissible speeds cause defacing of pier with various damage levels. Residual capacities of the affected pier are shown in Fig. 4a-d for the various impacts incurred from vehicles classes 5 to 8 respectively (shown in Table 1). Intersection points for individual cases between the shear and axial capacities show the concrete strength that optimizes the capacity of the pier in both flexure and shear.

Asides vehicle weights, the speeds of impact also affect the resulting residual capacities significantly. From the plots in Fig. 4 (a, b, c, and d), it can be surmised that increasing impact speed results in reduced residual capacity of the pier. A combination of large weight and high speed could lead to a total collapse of the RC pier (i.e., computed residual capacity of zero). This situation occurred at a vehicle speed of 45 mph (27.96 km/hr) when using vehicle classes 7 and 8, which is why their respective figures only show the trends of residual capacities up to 40 mph (24.85 km/hr). In designing an RC pier to withstand vehicular impact, the shear capacity is key. However, the shear capacity is inversely proportional to the axial capacity, as both reflect the compressive strength of the concrete in diametrically opposite ways. As such, a good tradeoff for balancing both characteristics is utilizing a compressive strength where these two capacities intersect, expressed in the figures as an inflection point. From the Fig. 4a-d, the inflexion points seem constant at 6 ksi (41.36 MPa). This indicates that an optimal compressive strength of concrete for resisting flexure and shear simultaneously in pier after undergoing vehicle impact is about 6 ksi (41.36 MPa).

Although the damage index ratio is used to modify the structural capacity of damaged piers post impact, this factor does not adequately capture inherent uncertainties that may exist in the impact scenario including inexactitudes in the mass and velocity measurements and geometrical and material parameters. Alternatively, a factor developed based on the resistance reduction method in structural reliability could be used in modifying the structural capacities.

4.2 Residual capacities using resistance reduction method

Alike the process used in estimating the reduced capacity of a RC pier after impact, the post impact axial and shear capacities of RC piers for different compressive strengths are computed using the resistance reduction factor. Figures 5 and 6 show the resulting residual axial and shear capacities for various impacting speeds at different concrete grades.

The graphed analytical results comparing both methods of adjusting the structural capacity of the pier after an impact event shown in Figs. 5 and 6 show very disparate predictions of the residual capacity of the pier. The damage index ratio factor (λ) seems to place less emphasis on the compressive strength as a factor in the axial capacity at increasing velocities. This is seen quite starkly in the residual axial capacities at 65 mph (40.38 km/hr), where the axial capacities are decreasing even at increasing compressive strengths. This can be attributed to the computation of the factor which is computed directly using the shear capacity. As such, the factor is biased by the behavior of the shear capacity at increasing compressive strengths even in computing the residual axial capacities. This is not the case with using the resistance

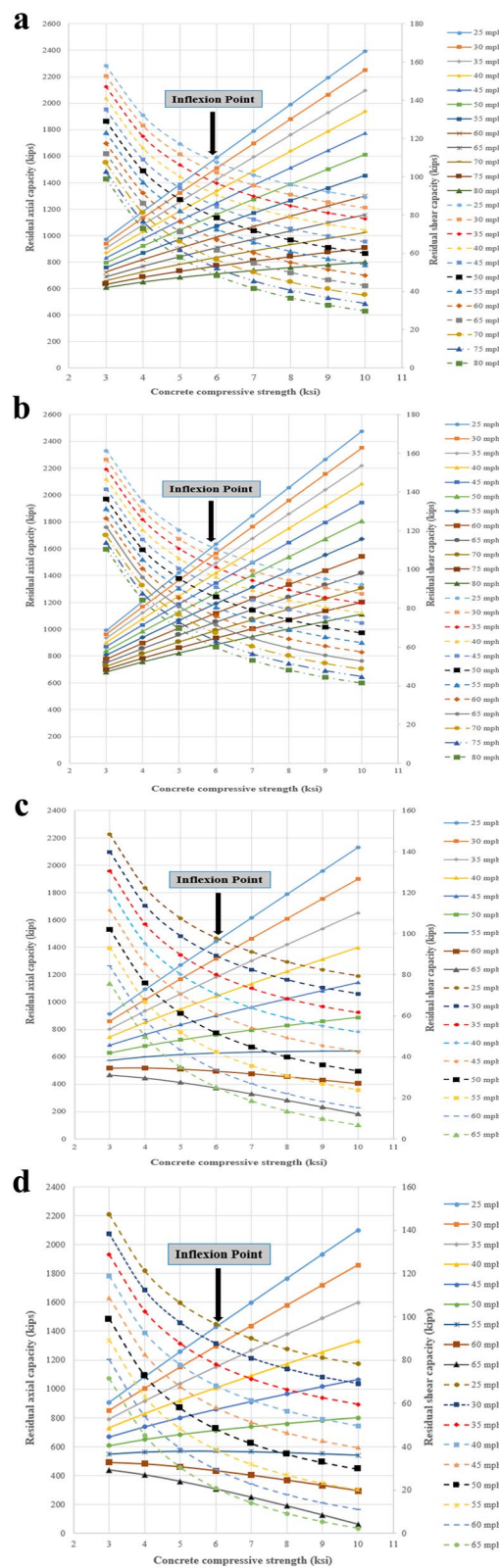


Fig. 4 **a.** Residual capacities showing inflexion point for Vehicle Class 5. **b.** Residual capacities showing inflexion point for Vehicle Class 6. **c.** Residual capacities showing inflexion point for Vehicle Class 7. **d.** Residual capacities showing inflexion point for Vehicle Class 8

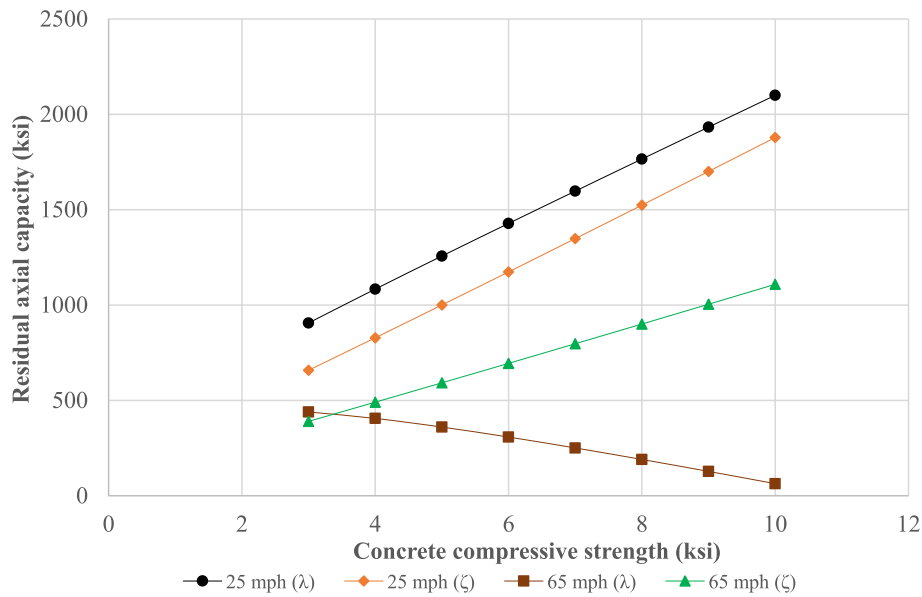


Fig. 5 Residual axial capacity using the damage index method and the resistance reduction method

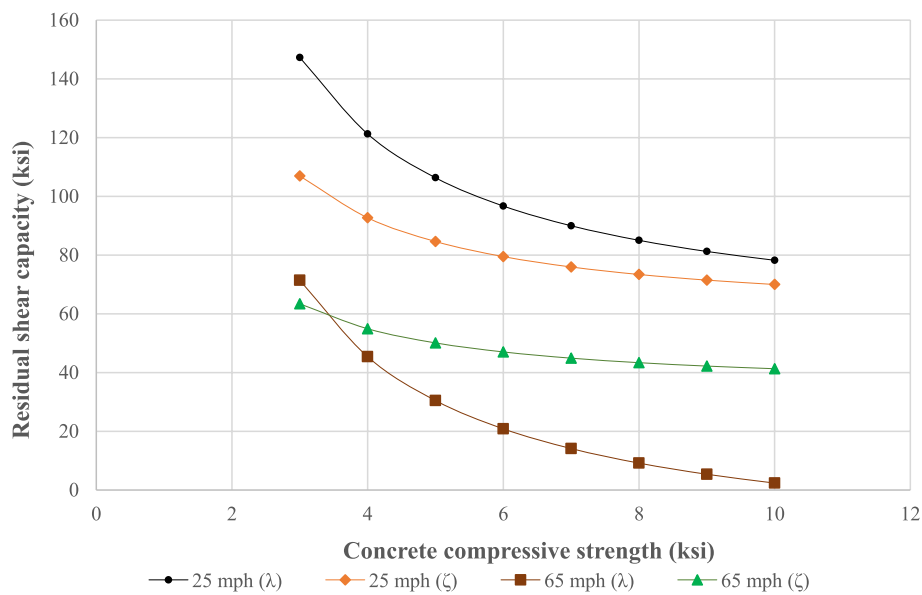


Fig. 6 Residual shear capacity using the damage index method and the resistance reduction method

reduction factor, as when utilizing a reliability-based computation, this factor weighs the contribution of the compressive strength alongside all other design variables. As a result, the factor is more representative of the contribution of all design variables and their uncertainties to the residual capacity of the pier both in axial and shear. The results of using the resistance reduction factor to compute the residual capacity of RC piers are shown in Fig. 7a-d for different vehicle weights (Vehicle Classes 5 to 8). Figure 7 (a, b, c and d) compares the resulting residual axial and shear capacities using both the methods.

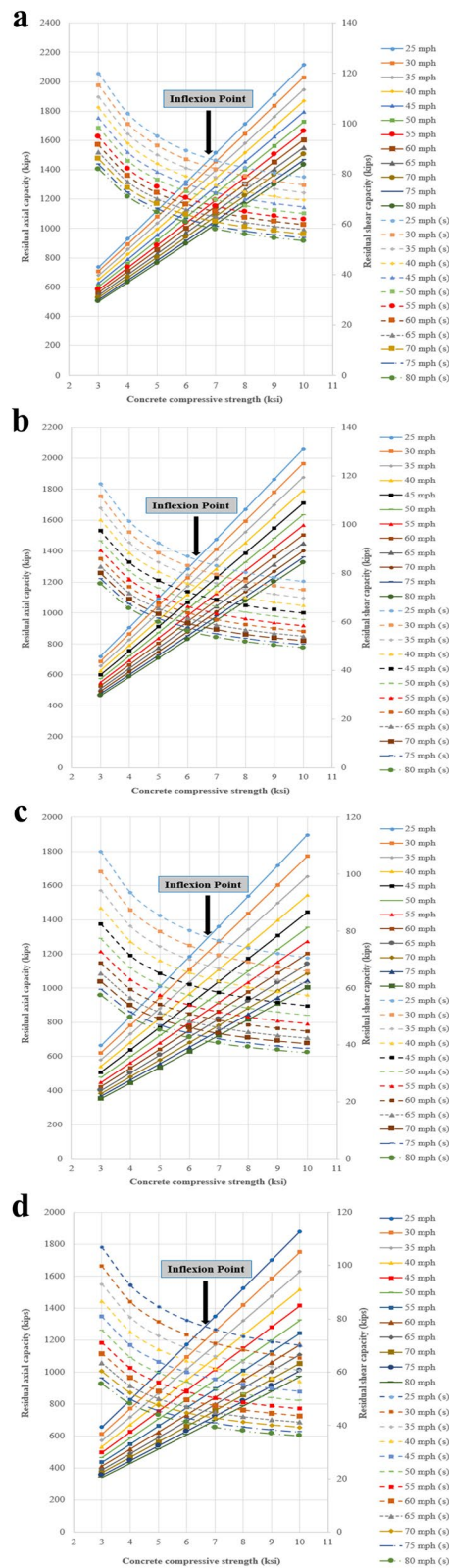


Fig. 7 **a.** Residual capacities showing inflexion points for Vehicle Class 5 using probability of failure (P_f). **b.** Residual capacities showing inflexion points for Vehicle Class 6 using probability of failure (P_f). **c.** Residual capacities showing inflexion points for Vehicle Class 7 using probability of failure (P_f). **d.** Residual capacities showing inflexion points Vehicle Class 8 using probability of failure (P_f)

From the analyses and as shown in Fig. 7 (a, b, c, and d), it can be surmised that as expected, there is a contrast in the relationship between axial capacity and compressive strength to that of shear strength and compressive strength. Increases in the compressive strength results in corresponding increases in the residual axial capacity and decreases correspondingly in the residual shear capacity. These phenomena can be attributed to the decreasing ductility of concrete with increasing compressive strength. These relationships hold across different impact scenarios including changing vehicle masses and speeds. These plots also indicate a compressive strength that would give a good tradeoff between both strength parameters. This tradeoff as indicated by the intersection points in the curves (about 7 ksi or 48.26 MPa) indicates a compressive strength that gives a balance between the axial and shear capacities. Lower compressive strengths will result in reduced axial capacities while increasing the shear capacity and vice versa. As such, a design compressive strength of around 7 ksi (48.26 MPa) might be a good tradeoff for ensuring an optimal balance in these strength parameters of interest using resistance reduction method.

4.3 Static bond strength and development length

Increased compressive strength due to the strain rate effect is produced in the concrete of RC pier while experiencing dynamic impact load. This dynamic compressive strength ($f'_{c,d}$) is determined by multiplying the compressive strength of concrete (f'_c) by the CDIF as shown in Eq. 25.

$$f'_{cd} = (CDIF) * f'_c \quad (25)$$

This change in the compressive strength will directly affect some of the pier's design specifications which are derivatives of the compressive strength including the bond strength and development length. The effect of this change in the compressive strength under the influence of dynamic loading on these design parameters is also investigated. The maximum bond stress u (psi) has been specified in Eq. 26 (Galambos and Ketter 1961), as:

$$u = 9.5 * (f'_c)^{\frac{1}{2}} / d_b \quad (26)$$

where: f'_c indicates the grade of concrete and d_b is the shear bar diameter (# 4) of 0.5 inch as per standard specification.

The recommended development length (l_d) considering interaction of different spalling initiated by splitting cracks and dynamic deformation is determined by Eq. 27 (Galambos and Ketter 1961).

$$l_d = 0.04 * A_b * f_y / (f'_c)^{\frac{1}{2}} \quad (27)$$

where: A_b represents the cross-sectional area of the main reinforcement (0.2 sq.-inch or 129.03 sq.-mm for # 4 ASTM steel rebar), f_y is the static yield strength of steel (60 ksi or 413.68 MPa) and f'_c indicates the grade of concrete.

By replacing the compressive strengths with the dynamic compressive strength, the bond strength of the structural member and the required development length under impact loading can be determined directly from the dynamic counterparts of the Eqs. 26

and 27 into the Eqs. 28 and 29 respectively. To determine dynamic bond strength and corresponding compressive concrete strength required for dynamic impact, dynamic compressive strength of concrete plays a significant role, and hence can be evaluated from direct correlation of the static counterpart. These equations will provide capturing the dynamic demand from static counterparts.

$$u_{dyn} = 9.5 * (f'_{cd})^{\frac{1}{2}} / d_b \quad (28)$$

$$l_{d,dyn} = 0.04 * A_b * \sigma_{dyn} / (f'_{c,d})^{\frac{1}{2}} \quad (29)$$

where: u_{dyn} and $l_{d,dyn}$ are bond strength and development length for dynamic impact, and the strength of steel rebar considered at dynamic condition during elastic–plastic state (σ_{dyn}) is considered from published journal as 68.1 ksi (68,100 psi or 0.4695 MPa) (Shi et al. 2008).

Accordingly, this increase in the compressive strength when the pier is under dynamic loading leads to an increase in the bond strength and concurrent decrease in the required development length as shown in the Figs. 8 and 9. This relationship also corroborates the increased shear strength of the concrete at specific vehicle impact load.

Static requirements comprising bond strength and development length are compared with the dynamic requirements as shown in the Figs. 8 and 9. The bond strength of the reinforced concrete member increases with the increase in the compressive strength induced by the high strain rate of loading. This trend continues to hold across the different concrete compressive strengths analyzed, and is as shown in Fig. 8. However, there is a steady decrease in the change in bond strength as the compressive strength increases with a 35% change at 3 ksi (20.68 MPa) reducing to 11% change at 10 ksi (68.95 MPa) between the static and dynamic bond strengths.

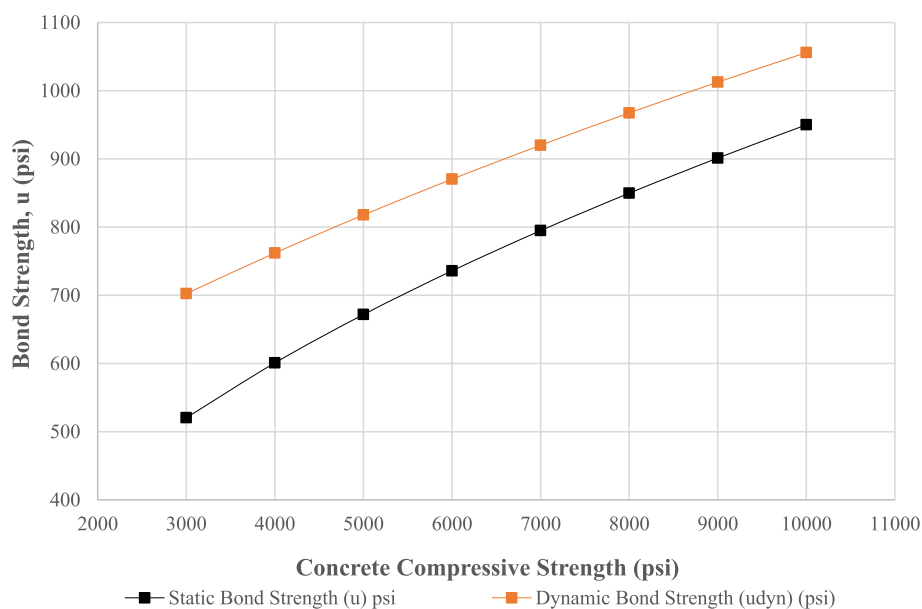


Fig. 8 Bond strength at increasing compressive strength

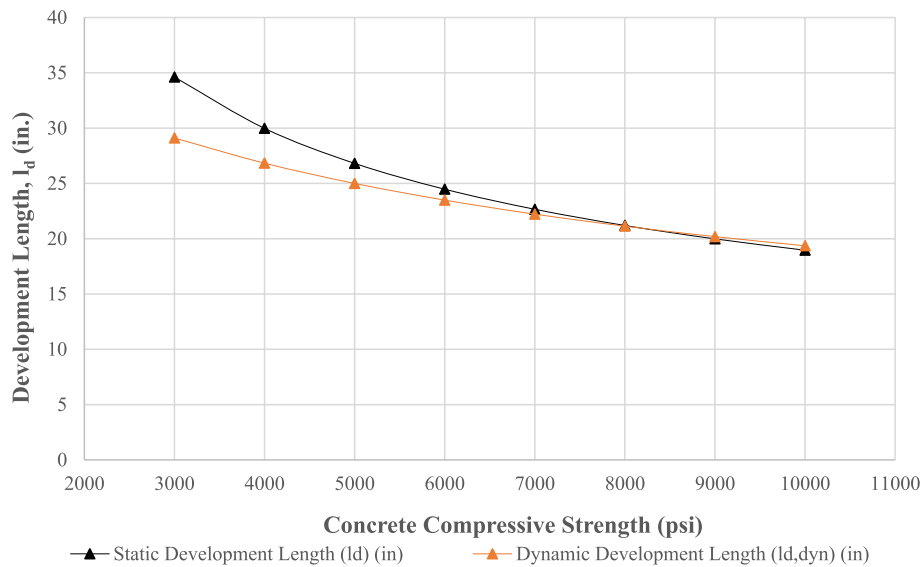


Fig. 9 Development length at increasing compressive strength

Similarly, the initial difference in the change in required development length progressively decreases with the required length 15% lower for dynamic loading than for static loading at 3 ksi (20.68 MPa) until the required length for the pier under dynamic loading is slightly higher than that for static loading for the 10 ksi (68.95 MPa) concrete compressive strength. These results indicate that the RC pier's ability to resist loads increases during impact events primarily due to the effect of the high strain rate of loading on the materials.

5 Discussion of results

This paper discusses the results of an analytical investigation into the effects of the dynamic increase factor on the residual capacity of a RC pier subjected to vehicular impact. Two methods of computing the post impact residual capacity were tested. The first, using the damage index method, involves computing a damage index as a ratio of the impact force to the shear capacity. This ratio is subtracted from one and used as a multiplier to reduce the structural capacities of the pier. The second method goes further in utilizing the damage index equation as a limit state equation to compute the probability of failure of the pier, and then uses this probability of failure to compute a resistance reduction factor. The resistance reduction factor is then used as a multiplier to reduce the design capacities, thus obtaining the residual capacities. The resistance reduction method was found to be slightly more conservative, estimating less residual capacity values at lower speeds. At higher speeds of 65 mph (40.38 km/hr) and beyond, however, the residual capacity proposed by the damage index diverged conspicuously from the trends at lower speeds, indicating a reduction in residual axial capacity with increasing compressive strength. This is in stark contrast to the expected static behavior of concrete and can be attributed to the nonlinear change in the shear strength with increasing compressive strength, leading to nonlinear changes in the damage index and by extension the residual capacity. This indicates that this

method might not accurately portray the behavior of the pier when hit with objects at high impact velocities. This drawback of the damage index is overcome in using the resistance reduction method, which in using a reliability analysis, accurately projects the influence of each design variable's contribution to the pier's resistance and as such is not unduly influenced by a single design parameter. Analyzing results for different speeds and different vehicle masses allowed for some conclusions to be drawn as to optimal compressive strengths of concrete to balance the paradoxical changes in axial and shear strength at changing compressive strengths. Results from the Figs. 4 and 7 indicate that in order to optimize the axial and shear capacities of an RC pier, concrete compressive strengths between 6 to 7 ksi (41.36 to 48.26 MPa) should be utilized to allow the pier resisting dynamic impact to retain some residual capacity and stay in service. As the compressive strength is a material property, the vehicle class has no effect on it. Furthermore, as the residual capacities are changing with changing the weights (vehicle class) and velocity of impact of vehicles, the intersection between the residual capacities stay constant at a specific compressive strength. This indicates that in order to design a column for vehicle impact, the inflexion point represents the good tradeoff between the compressive strength and resistance value where both the shear and axial capacities can be optimized for impact resistance. These results corroborate with the results from other perspectives such as energy methods, published in the existing literatures (Roy and Sorensen 2021b; a).

In addition, the change in the bond strength and consequently the development length due to a change in the compressive strength at high strain rates are also analyzed. It is noted that there is a significant increase in the bond strength under high strain rates compared to the bond strength under static loading conditions. This difference is quite significant at lower compressive strengths and gradually reduces with increasing compressive strength. A similar observation was found for the development length, with a decrease in the required development length at high strain rates compared to the requirement under static loading conditions. This difference in requirement decreases with increasing compressive strength becoming insignificant beyond 7 ksi (48.26 MPa). These observations indicate that the enhancement of the design properties of the RC pier due to increase in the compressive strength of the concrete at high strain rates, encapsulated in the DIF, gradually reduces and will at some point be negated at ultra-high compressive strengths, for example ultra-high-performance concrete (UHPC).

The dynamic over static bond stress ratios (u_{dyn}/u) and corresponding development length ratios ($l_{d,dyn}/l_d$) at various concrete compressive strengths (f'_c) are plotted and shown in Fig. 10. From Fig. 10, u_{dyn}/u and $l_{d,dyn}/l_d$ are showing second degree polynomial increasing and decreasing trends respectively according to the gradual increase in concrete compressive strengths, ranging from 3 to 10 ksi (20.68 to 68.95 MPa). This study proffers significant practical correlations that are summed up for encapsulating demand for dynamic bond strength and corresponding development length in order for safely withstanding vehicle impact loading by the concrete pier. As an outcome of this study using regression analyses, two corresponding relationships comprising dynamic bond strength and development length, as shown in the Fig. 10, are presented in the Eqs. 30 and 31. These equations will help to determine the dynamic demands comprising bond strength and development length from their corresponding static counterparts.

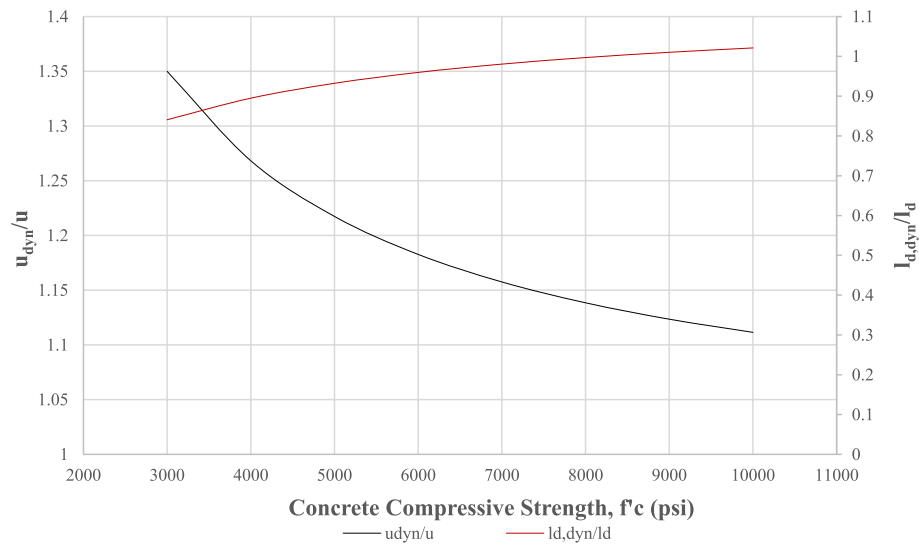


Fig. 10 Bond stresses and development length's ratios at corresponding concrete compressive strength

$$u_{dyn} = u \cdot [-3.10^{-9}(f'_c)^2 + 7.10^{-5}(f'_c) + 0.6745] \quad (30)$$

$$l_{d,dyn} = l_d \cdot [5.10^{-9}(f'_c)^2 - 0.0001(f'_c) + 1.5869] \quad (31)$$

where: u_{dyn} and $l_{d,dyn}$ are the dynamic bond strength and development length demand for dynamic load, u and l_d are the static counterparts representing bond strength and development length, and f'_c is the compressive strength of concrete in expressed in psi.

6 Conclusions

This research offers an insight into quantifying the severity of damage to the impacted RC piers exposed to vehicle collision. This approach conservatively examines concrete of a bridge pier as the primary material in resisting vehicular impact. An optimal concrete strength to resist vehicle impact is determined by using the damage index method. Similarly, an optimal concrete strength is determined via a resistance reduction factor, computed using reliability analysis. The resistance reduction factor is then used as a multiplier to reduce the design capacities, thus obtaining the residual capacities. This study can serve as an important tool for practitioners and aid to forensic structural engineers in scrutinizing the post impact serviceability as well as performance studies of concrete used in bridge piers. Some conclusions that can be drawn from the analyses carried out to determine vehicle impacted residual capacity subjected to concrete strength, include:

Concrete compressive strengths between 6 to 7 ksi (41.36 to 48.26 MPa) should be utilized to allow the RC pier to safely resist vehicle impact.

The post impact pier performance is further scrutinized using bond strength. It has been put down that there is a significant increase in the bond strength when subjected to dynamic loading conditions compared to bond strength under static loading conditions. This difference gradually decreases with the increase in compressive strength.

Accordingly, the change in bond strength leads to changes in the required development length, with a decrease in the required development length at high strain rates compared to the requirement under static loading conditions. This difference in requirement decreases with increasing compressive strength and is inconsequential beyond 7 ksi (48.26 MPa).

Dynamic demands for bond strength and development length can be computed by using the Eqs. 30 and 31 from their corresponding static counterparts and concrete compressive strength to safely withstand specific vehicle impact load by the traditional RC pier.

7 Symbols:

f_{cd} Dynamic compressive strength at the dynamic strain rate.

$\dot{\epsilon}_d$ Dynamic strain rate of concrete.

f_{cs} Static compressive strength as quasi-static strain rate.

$\dot{\epsilon}$ Quasi-static strain rate at concrete.

DIF Dynamic increase factor.

CDIF Dynamic increase factor for concrete in a compression.

α Dynamic constant.

f_{cu} Cube compressive strength.

M Weight of semi-trailer vehicle.

V Impact velocity.

F_{max} Frontal impact force.

t Duration of impact.

E Total impact energy.

I_r Frontal shock (force) due to vehicle impact.

$I_{r,max}$ Frontal overpressure.

t_d^+ Positive phase for impact pressure.

γ Decay co-efficient of the waveform.

I_{dyn} Dynamic impact force.

λ Damage index.

f_c' 28 days' compressive strength of concrete,

σ_o Yield strength of steel.

A_g Gross cross-sectional area of concrete and.

A_s Total cross-sectional area of longitudinal steel.

P Transverse steel ratio.

V_c Shear strength carried by concrete.

V_s Transversal shear capacity.

v_b Shear constant.

A_h Area of single hoop for transverse steel.

ρ_l Longitudinal steel ratio.

D Spiral diameter of transversal steel.

σ_{yh} Yield stress of transverse steel.

u Maximum bond stress.

u_{dyn} Maximum bond stress.

d_b Bar diameter.

l_d Development length.

$l_{d,dyn}$ Demand for development length at impact.

f_y Static yield strength of steel.

P_f Probability of failure.

β Reliability index.

Φ Reliability function.

Φ^{-1} Inverse of the tail probability function.

E_c Elastic modulus of concrete.

$f'_{c,d}$ Dynamic compressive stress of concrete.

Conversion Chart for the US Customary to the Equivalent SI Units.

US Customary	SI Unit
1 ksi	6.89 MPa (kN/mm ²)
1 psi	0.00689 Mpa (kN/mm ²)
1 kip-in	0.113 kN-m
1 kip	4.45 kN
1 lbs	0.00445 kN
1 mph	1.61 km/hr
1 ft-lb/sec	0.00136 kN-m/sec (1.36 N-m/sec)
1 in	0.0254 m (25.4 mm)

Acknowledgements

This publication was supported by a subcontract from Rutgers University, Center for Advanced Infrastructure and Transportation (CAIT), under DTFH62-08-C-00005 from the U.S. Department of Transportation-Federal Highway Administration (USDOT-FHWA). Any opinions, findings, and conclusions or recommendations expressed in this publication are those of the author(s) and do not necessarily reflect the views of Rutgers University or those of the U.S. Department of Transportation-Federal Highway Administration.

Author's contributions

Suman Roy*¹: Conceptualized and developed the theoretical formalism, analytical models and simulations, validation, performed the analytic calculations, and writing draft. Ikwulono D. Unobe¹: Apprehended the analytical calculations, performed the analytical simulations, and edited the draft. Andrew D. Sorensen¹: Conceptualized and overall guidance, editing manuscript and supervised the project. All authors have read and approved the manuscript.

Funding

¹). Center for Advanced Infrastructure and Transportation (CAIT), under DTFH62-08-C-00005 from the U.S. Department of Transportation-Federal Highway Administration (USDOT-FHWA).

Availability of data and materials

Some or all data, models, or code that support the findings of this study are available from the corresponding author upon reasonable request.

Declarations

Competing interests

We, the authors of the manuscript declare that we have no competing interests.

Received: 8 September 2022 Accepted: 9 October 2022

Published online: 02 November 2022

References

- AASHTO (2011) Guide Specifications for LRFD Seismic Bridge Design, 2nd Edition. American Association of State Highway and Transportation Officials. American Association of State Highway and Transportation Officials, Washington, DC
- AASHTO M145–91 (2008) "American Association Of State Highway And Transportation Officials." Classification of Soils and Soil-Aggregate Mixtures for Highway Construction Purposes, 9
- ACI (2011) ACI 318–11: Building Code Requirements for Structural Concrete. American Concrete Institute
- ACI committee 318 (1985) Building code requirements for structural plain concrete (ACI 318.1-83) and commentary. Int J Cement Composites and Lightweight Concrete. 7(1):60
- AFDC (2018) "Vehicle Weight Classes & Categories." Alternative Fuels Data Centre, U.S. Department of Energy.

- Ameli MJ, Pantelides CP (2017) Seismic analysis of precast concrete bridge columns connected with grouted splice sleeve connectors. *J Struct Eng Am Soc Civil Eng* 143(2):4016176
- Auyeung S, Alipour A, Saini D (2019) Performance-based design of bridge piers under vehicle collision. *En Struct, Elsevier* 191:752–765
- Ayyub BM, McCuen RH (2016) Probability, statistics, and reliability for engineers and scientists. CRC Press
- Bathurst RJ, Allen TM, Nowak AS (2008) Calibration concepts for load and resistance factor design (LRFD) of reinforced soil walls. *Can Geotech J* 45(10):1377–1392
- Cao R, Agrawal AK, El-Tawil S, Xu X, Wong W (2019) Heavy Truck Collision with Bridge Piers: Computational Simulation Study. *J Bridge Eng Am Soc Civil Eng* 24(6):4019052
- Cook W (2014) "Bridge Failure Rates, Consequences, and Predictive Trends." All Graduate Theses and Dissertations, 116.
- Der Kiureghian A (2008) Analysis of structural reliability under parameter uncertainties. *Probab Eng Mech* 23(4):351–358
- Engineers A S of C (2013) "Minimum Design Loads for Buildings and Other Structures (ASCE/SEI 7–10)." American Society of Civil Engineers.
- Feyerabend M (1988) Hard transverse impacts on steel beams and reinforced concrete beams. University of Karlsruhe (TH), Germany
- Galambos T V, Ketter R L (1961) "Columns under combined bending and thrust, Proc. ASCE, 85 (EM2), p. 1,(1959),(also ASCE Trans. Vol. 126,(1961), Reprint No. 136 (61–22)."
- Gomez NL, Alipour A (2014) Study of circular reinforced concrete bridge piers subjected to vehicular collisions. *Struct Congress 2014:577–587*
- Hwang E, Nowak AS (1991) Simulation of Dynamic Load for Bridges. *J Struct Eng* 117(5):1413–1434
- Joshi AS, Gupta LM. A simulation study on quantifying damage in bridge piers subjected to vehicle collisions. *Int J Adv Struct Eng.* 2012;4(1):1–13.
- Kowalsky MJ (2000) Deformation limit states for circular reinforced concrete bridge columns. *J Struct Eng Am Soc Civil Eng* 126(8):869–878
- Malvar L J, Crawford J E (1998) Dynamic increase factors for concrete. Naval Facilities Engineering Service Center Port hueneme CA.
- Mander JB, Priestley MJ, Park R (1988) Theoretical stress-strain model for confined concrete. *J Struct Eng (United States)* 114(8):1804–1826
- Nowak AS, Collins KR (2012) Reliability of structures. CRC Press
- Roy S, Unobe I, Sorensen AD (2021) Vehicle-Impact Damage of Reinforced Concrete Bridge Piers: S State-of-the Art Review. *J Perform Constr Facil.* 35(5):03121001 (American Society of Civil Engineers 2021)
- Roy S, Unobe ID, Sorensen AD (2022) Reliability assessment and sensitivity analysis of vehicle impacted reinforced concrete circular bridge piers. *Structures, Elsevier* 37:600–612
- Roy S, Sorensen A (2021a) "Energy Based Model of Vehicle Impacted Reinforced Bridge Piers Accounting for Concrete Contribution to Resilience." 18th International Probabilistic Workshop: IPW 2020, Springer Nature, 301.
- Roy S, Sorensen A (2021b) "A Reliability Based Crack Propagation Model for Reinforced Concrete Bridge Piers Subject to Vehicle Impact." 18th International Probabilistic Workshop: IPW 2020, Springer Nature, 95.
- Schultz GG, Seegmiller L (2006) Utah Commercial Motor Vehicle Weigh-in-Motion Data Analysis and Calibration Methodology
- Sharma H, Hurlbaas S, Gardoni P (2012) Performance-based response evaluation of reinforced concrete columns subject to vehicle impact. *Int J Impact Eng* 43:52–62
- Shi Y, Hao H, Li Z-X (2008) Numerical derivation of pressure–impulse diagrams for prediction of RC column damage to blast loads. *Int J Impact Eng Elsevier* 35(11):1213–1227
- Spyrakos CC, Vlassis AG (2003) Seismic retrofit of reinforced concrete bridges. *WIT Transactions on the Built Environment, WITPress* 72:79–88
- Thomas RJ, Steel K, Sorensen AD (2018) Reliability analysis of circular reinforced concrete columns subject to sequential vehicular impact and blast loading. *Eng Struct Elsevier* 168:838–851
- Vrouwenvelder T (2000) Stochastic modelling of extreme action events in structural engineering. *Probab Eng Mech* 15(1):109–117
- Wardhana K, Hadipriono FC (2003) Analysis of recent bridge failures in the United States. *J Perform Construct Facil Am Soc Civil Eng* 17(3):144–150
- Zhou D, Li R (2018a) Damage assessment of bridge piers subjected to vehicle collision. *Adv Struct Eng* 21(15):2270–2281
- Zhou D, Li R (2018b) Damage assessment of bridge piers subjected to vehicle collision. *Adv Struct Eng* 21(15):2270–2281 (SAGE Publications Sage UK: London, England)

Publisher's Note

Springer Nature remains neutral with regard to jurisdictional claims in published maps and institutional affiliations.